

Hemodynamic measurements from individual blood cells in early mammalian embryos with Doppler swept source OCT

Irina V. Larina,¹ Steven Ivers,² Saba Syed,² Mary E. Dickinson,¹ and Kirill V. Larin^{2,*}

¹Molecular Physiology and Biophysics, Baylor College of Medicine, One Baylor Plaza, Houston, Texas 77584, USA

²Biomedical Engineering Program, University of Houston, N207 Engineering Building 1, Houston, Texas 77204, USA

*Corresponding author: klarin@uh.edu

Received November 17, 2008; revised February 11, 2009; accepted February 18, 2009;
posted February 23, 2009 (Doc. ID 104197); published March 20, 2009

The most common and lethal birth defects affect the cardiovascular (CV) system. The mouse is a superior model for identifying and understanding mammalian CV birth defects, but there is a great need for tools that can detect early and subtle deficiencies in cardiac function in mouse embryos. We combined swept source optical coherence tomography (SS-OCT) with live mouse embryo culture protocols to generate structural two-dimensional and three-dimensional imaging and hemodynamic measurements in a live 8.5 day embryo just a few hours after the beginning of a heartbeat. Our data show that individual circulating blood cells can be visualized with structural SS-OCT, and using Doppler SS-OCT the velocity of single moving blood cells were measured during different phases of the heartbeat cycle. These results demonstrate that Doppler SS-OCT is an extremely useful tool for structural and hemodynamic analysis at the earliest stages of mammalian blood circulation. © 2009 Optical Society of America

OCIS codes: 110.4500, 170.4500, 170.6920, 180.1655, 280.3340.

There is a great need for tools to characterize dynamic aspects of mammalian embryonic cardiovascular (CV) development in mutant embryos to reveal the genetic basis of functional deficiencies. Recent advances in optical coherence tomography (OCT) have rapidly led to the application of this exciting imaging modality for live imaging of embryonic cardio dynamics and blood flow in *Drosophila* [1], *Xenopus laevis* [2,3], quail [4], and chick [5]. Despite the obvious need to address questions regarding mammalian embryonic development, there have been only a few OCT studies. Jenkins *et al.* [6] performed three-dimensional (3D) OCT imaging of excised and externally paced beating embryonic mouse hearts at 13.5 dpc. Luo *et al.* [7] reported imaging of beating 10.5 dpc hearts in embryos that were maintained outside the uterus, but the heartbeat was significantly slower than normal. Our group has previously developed protocols for maintenance and the growth of 5.5–10.5 dpc mouse embryos in static culture [8] and has successfully applied these protocols for characterization of blood flow phenotypes using confocal microscopic imaging [9]. Recently, we combined Doppler swept source optical coherence tomography (SS-OCT) analysis with mouse embryo culture protocols for live 3D embryonic imaging and reconstructed spatially and temporally resolved Doppler shift velocity profiles from deep 9.5 dpc embryonic vessels in which flow is well established [10].

In this Letter, we applied Doppler SS-OCT to perform hemodynamic measurements at an earlier embryonic stage, 8.5 dpc, just a few hours after the beginning of a heartbeat when blood circulation first begins. At this stage, the majority of blood cells are still found in the blood islands with limited numbers

of circulating erythroblasts [9]. Thus, we focused this Letter on OCT signal detection from single circulating blood cells.

The experimental SS-OCT setup was similar to the system described in [10]. Briefly, the system utilizes a broadband swept source laser (Thorlabs, SL1325-P16) centered at $\lambda_0 = 1325$ nm with the spectral width of $\Delta\lambda = 100$ nm and an output power of 12 mW. The scan repetition rate over the full operating wavelength range is 16 kHz. The OCT system is based on a Mach-Zender interferometer (MZI) with 10% of the power going to the reference arm and 90% to the sample arm. The interference fringes are detected by a balanced photodetector (Thorlabs, PDB140C), digitized using a 14 bit analog-to-digital converter and recalibrated using an MZI clock signal. The full imaging depth is 3 mm in air and about 2.2 mm in tissue, which is sufficient to image a whole mouse embryo with an extra embryonic yolk sac (less than 2 mm). For embryo imaging, the scanning head of the SS-OCT system was positioned inside a commercial 37 °C CO₂ incubator.

Blood flow velocity at each pixel was reconstructed according to the formula [11]

$$v = \Delta\phi / (2n\langle k \rangle \tau \cos(\beta)), \quad (1)$$

where $\Delta\phi$ is a Doppler shift-induced phase shift calculated between successive A-scans, n is a refractive index, $\langle k \rangle$ is the average wavenumber, τ is the time between the successive A-scans, and β is an angle between the flow direction and the laser beam. The angle β was calculated from structural two-dimensional (2D) and 3D data sets acquired from the embryo; the refractive index was assumed as $n = 1.4$.

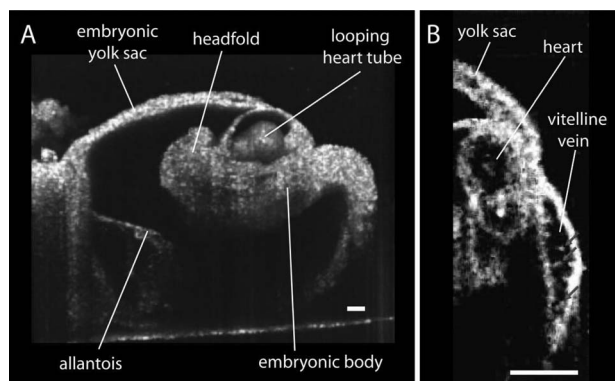


Fig. 1. Live structural imaging of 8.5 day mouse embryo with SS-OCT. A, Typical 3D reconstruction of the whole embryo with the yolk sac. B, SS-OCT image depicting a cross section of a heart and a fragment of vitelline vein with individual circulating blood cells. The scale bars correspond to 100 μm .

To correct for the bulk tissue movement, the average Doppler shift value from the surrounding embryonic tissue was subtracted from the blood cell velocity measurements. Doppler measurements were previously validated by measuring the flow of milk controlled by a syringe pump through a flow chamber in the range from 0 to 7.0 mm/s with the standard deviation of ± 0.1 mm/s (data not shown).

Wild type CD-1 male and female mice (Charles River Laboratories, Wilmington, Mass.) were mated overnight. Females were examined for vaginal plugs daily, and the presence of a plug was taken as 0.5 dpc. Embryos were dissected with the yolk sac intact at 8.5 dpc in the preheated to 37°C dissecting medium consisting of 89% DMEM/F12, 10% FBS, and 1% 100X Pen-strep solution (Invitrogen, Grand Island, N.Y.). The dissection and imaging stations were heated and maintained at 37°C using a custom made heater box and a conventional heater. Dissected embryos were transferred to a 37°C, 5% CO₂ incubator for at least 1 h for recovery. The imaging was performed for up to 4 h after the dissection.

Figure 1A shows a cross section from a 3D reconstruction of a live 8.5 dpc mouse embryo acquired with SS-OCT. The reconstruction is performed from 512×512 in depth A-scans. Embryonic structures are clearly distinguishable in the reconstruction, and the

whole embryo is within the imaging depth of the system. Figure 1B shows a higher resolution view through the heart and vitelline vein of the embryo. In this image, individual circulating blood cells are clearly visible in the vitelline vein (labeled by arrows) and the heart. Although we can detect single blood cells and the frame rate of the system is sufficient to follow their movement, we found it technically difficult to orient the imaging plane so as to capture the 3D trajectory of the moving cells and to determine cell velocity by direct cell tracking.

To circumvent this limitation, structural imaging was combined with an SS-OCT Doppler shift detection for hemodynamic measurements. Figure 2A shows a structural image of the dorsal aorta within the embryo. Color coded Doppler velocity maps acquired at different phases of the heartbeat cycle from the same area of the embryo are also shown. The Doppler velocity images were taken at 512 A-scans per frame at 25 fps. Different colors indicate different velocities with green corresponding to zero as indicated by the rainbow scale. The area of the dorsal aorta where measurements were performed is outlined on the images. A higher magnification view of the same area is shown in Fig. 2B. A Doppler shift signal from a small group of cells as well as individual circulating blood cells are clearly distinguishable in the images. Doppler velocities from all individual detectable cells in the area outlined in Fig. 2A were measured for each acquired Doppler time frame in the time lapse. Figure 3A shows an average blood flow velocity plotted versus time. Dynamics of the blood flow velocity in time reveals the pulsatile nature of the flow and allows analyzing hemodynamic changes during the heartbeat. The heart rate (about two beats per second) correlates well with previously reported measurements at this embryonic stage, and the flow velocity values acquired in the dorsal aorta are similar to published blood flow measurements in the yolk sac at the same embryonic stage [12], supporting the physiological relevance of these data.

To reconstruct blood flow velocity profiles across the same vessel at different phases of the heartbeat cycle, we analyzed individual time frames and measured the Doppler velocity shift from each visible blood cell and the distance of the blood cell to the vessel wall. The data points for each time frame were re-

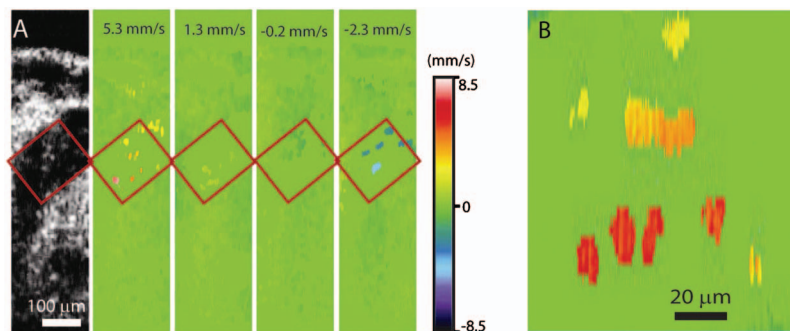


Fig. 2. Doppler OCT velocity signals from blood cells on the embryonic day 8.5. A, Structural and corresponding color coded Doppler velocity images acquired at different phases of the heartbeat cycle. Green corresponds to zero velocity. Individual blood cells are distinguishable in the dorsal aorta. B, Magnified view of the same area showing Doppler signal from single cells as well as a small group of cells.

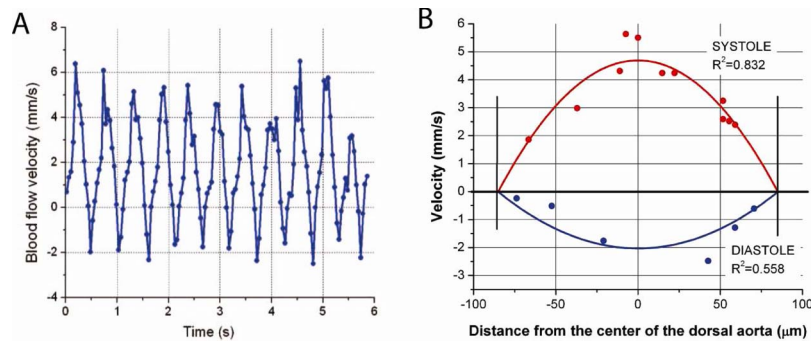


Fig. 3. (Color online) Blood flow measurements at different phases of the cardiac cycle. A, Average blood flow velocity as a function of time in the corresponding area of the dorsal aorta. Each data point corresponds to the Doppler OCT velocity measurement from an individual cell. The data points were regressed using a parabolic fit. B, Blood flow velocity profiles. Each data point corresponds to the Doppler OCT velocity measurement from an individual cell. The data points were regressed using a parabolic fit.

gressed by a parabolic fit. Figure 3B shows the data points and the corresponding fits for different phases of the cardiac cycle. Even though the profiles were reconstructed from a very limited number of cells, it is clear that cell velocity is greater in the center of the vessel than near the vessel wall, and the measurements fit well with the parabolic profile suggesting that laminar flow is present. Our measurements show that even without the application of additional image processing algorithms SS-OCT can provide sensitive spatially resolved hemodynamic measurements at the earliest stages of blood circulation.

Hemodynamic measurements in early mouse embryos can be performed with subcellular resolution by fast scanning confocal microscopy of fluorescently labeled blood cells; however, the imaging depth of this technique is limited (200–300 μm), which does not allow imaging of deep embryonic vessels. On the other hand, high frequency ultrasound has a high imaging depth but lacks spatial resolution (30–50 μm). OCT is an excellent compromise providing reasonable depth penetration (about 2 mm) and single cell resolution. These properties have enabled us to make sensitive flow measurements from single cells deep within the embryonic circulatory system.

This Letter, for the first time to our knowledge, shows that velocity measurements from individual circulating blood cells can be acquired from deep embryonic vessels in early mammalian embryos at the onset of circulation. The combination of Doppler SS-OCT and a live embryo culture has great potential as a routine screening tool for mouse mutants with impaired cardiology. Such highly sensitive methods to assess function can provide a greater understanding of how birth defects arise and how subtle birth defects relate to CV failure later in life.

The authors would like to thank Mohamad Ghosn and Narendran Sudheendran (University of Houston) for technical assistance and Ross Poché (Baylor

College of Medicine) for a critical reading of this Letter. This study was supported, in part, by Postdoctoral Fellowship from the American Heart Association (I. V. Larina), and grants from the National Institutes of Health (NIH) (HL077187 MED), W. Coulter Foundation, and Office of Naval Research (ONR) (K. V. Larin).

References

1. M. A. Choma, S. D. Izatt, R. J. Wessells, R. Bodmer, and J. A. Izatt, *Circulation* **114**, e35 (2006).
2. A. Mariampillai, B. A. Standish, N. R. Munce, C. Randall, G. Liu, J. Y. Jiang, A. E. Cable, I. A. Vitkin, and V. X. D. Yang, *Opt. Express* **15**, 1627 (2007).
3. S. A. Boppart, G. J. Tearney, B. E. Bouma, J. F. Southern, M. E. Brezinski, and J. G. Fujimoto, *Proc. Natl. Acad. Sci. U.S.A.* **94**, 4256 (1997).
4. M. W. Jenkins, O. Q. Chughtai, A. N. Basavanahally, M. Watanabe, and A. M. Rollins, *J. Biomed. Opt.* **12**, 030505 (2007).
5. M. W. Jenkins, D. C. Adler, M. Garghesha, R. Huber, F. Rothenberg, J. Belding, M. Watanabe, D. L. Wilson, J. G. Fujimoto, and A. M. Rollins, *Opt. Express* **15**, 6251 (2007).
6. M. W. Jenkins, F. Rothenberg, D. Roy, V. P. Nikolski, Z. Hu, M. Watanabe, D. L. Wilson, I. R. Efimov, and A. M. Rollins, *Opt. Express* **14**, 736 (2006).
7. W. Luo, D. L. Marks, T. S. Ralston, and S. A. Boppart, *J. Biomed. Opt.* **11**, 021014 (2006).
8. E. A. V. Jones, D. Crotty, P. M. Kulesa, C. W. Waters, M. H. Baron, S. E. Fraser, and M. E. Dickinson, *Genesis* **34**, 228 (2002).
9. J. L. Lucitti, E. A. V. Jones, C. Huang, J. Chen, S. E. Fraser, and M. E. Dickinson, *Development* **134**, 3317 (2007).
10. I. V. Larina, N. Sudheendran, M. Ghosn, J. Jiang, A. Cable, K. V. Larin, and M. E. Dickinson, *J. Biomed. Opt.* **13**, 060506 (2008).
11. B. Vakoc, S. Yun, J. de Boer, G. Tearney, and B. Bouma, *Opt. Express* **13**, 5483 (2005).
12. E. A. V. Jones, M. H. Baron, S. E. Fraser, and M. E. Dickinson, *Am. J. Physiol. Heart Circ. Physiol.* **287**, H1561 (2004).